Advanced Composite Materials
Publication details, including instructions for authors and subscription information:
http://www.tandfonline.com/loi/tacm20

Probabilistic-statistical approach to the mechanical behavior of ceramic matrix composites (CMCs)

J. Lamon [a]

[a] Laboratory for Thermostructural Composites, UMR-5801 (CNRS-SEP/SNECMA-UB1), University of Bordeaux-1, 3 Allée de La Boétie, 33600 Pessac, France

Version of record first published: 02 Apr 2012.

Adv. Composite Mater., Vol. 8, No. 1, pp. 97–106 (1999)

Probabilistic-statistical approach to the mechanical behavior of ceramic matrix composites (CMCs)

J. LAMON

Laboratory for Thermostructural Composites, UMR-5801 (CNRS-SEP/SNECMA-UB1), University of Bordeaux-1, 3 Allée de La Boétie, 33600 Pessac, France

Abstract—The approach to the mechanical behavior of CMCs that is proposed, is based on a statistical-probabilistic description of multiple matrix cracking and fiber failures. It is applied to unidirectional and woven SiC/SiC composites. The predicted stress–strain behaviors were in good agreement with available experimental data. The influence of various factors including porosity, loading conditions and constituent properties is anticipated.

Keywords: Ceramic matrix composite; mechanical behavior; damage; fracture probability; failure; statistics.

1. INTRODUCTION

Ceramic matrix composites combine brittle materials including the fiber and the matrix. Nevertheless they are capable of a highly non-linear stress–strain behavior reflecting damage tolerance. Damage involves multiple microcracks or cracks that form in the matrix and then are arrested by the fibers. The ultimate failure occurs when a critical number of fibers have failed. Matrix cracking and fiber failures are brittle failure phenomena. They are initiated by microstructural heterogeneities distributed randomly in the matrix and in the fibers.

Fracture-statistics based approaches are appropriate for modeling the defect-induced failures of brittle materials. Several approaches to brittle fracture have been proposed in the literature. The Weibull model provides a satisfactory approximation in the presence of uniaxial stress states. More fundamental approaches such as the Multiaxial Elemental Strength Model are required for complex shapes subject to multiaxial stress states [1]. Damage and failure models based upon statistical approaches to brittle failure have been developed to predict the ultimate strength [2–5] and the stress–strain behavior [6, 7] of unidirectionally reinforced CMCs subject to tensile loads, and the scenario of matrix damage in 2D woven SiC/SiC composites [8].

The paper presents damage and failure models based upon statistical approaches to brittle failure to predict the stress–strain behavior of composites at various scales, including microcomposites (elementary scale) [6], minicomposites (intermediate scale) [7] and 2D woven composites [8]. A microcomposite consists of a concentric cylinder element containing a single fiber with a coating (i.e. interphase) plus a matrix annulus. This specimen is appropriate for designing interphases [9]. Microcomposites are not examined in the paper. A minicomposite is a bundle of parallel fibers coated with a layer of interfacial material and a matrix. Minicomposites are representative of the matrix infiltrated bundles in textile ceramic matrix composites reinforced with fabrics of woven bundles.

2. APPROACHES TO MATRIX CRACKING AND ULTIMATE FAILURE IN MINICOMPOSITES

2.1. Matrix cracking

As matrix cracking proceeds in a minicomposite specimen loaded in tension parallel to the fiber axis, the matrix becomes subdivided into smaller and smaller fragments. A fragment is defined as the uncracked element bounded by two transverse matrix cracks (Fig. 1).

Matrix cracking is modelled as the brittle failure of uncracked fragments. This approach differs from the conventional one developed for fiber fragmentation, which considers the whole cracked volume. The probability of failure of a fragment is obtained from integration of the 2-parameter Weibull equation, for the specific stressfield operating on the matrix.

In the presence of n matrix cracks, the matrix is subdivided into $(n+1)$ fragments (Fig. 1). The probability of brittle failure of the ith matrix fragment of length $2l_i$ is given by the following equation:

$$P_{\mathrm{Mi}} = 1 - \exp\left[-2S_{\mathrm{M}} \cdot \int_0^{l_i} \left(\frac{\sigma_{\mathrm{M}}}{\sigma_{0\mathrm{M}}}\right)^{m_{\mathrm{M}}} \mathrm{d}x\right], \tag{1}$$

where S_{M} is the cross-sectional area; m_{M} and $\sigma_{0\mathrm{M}}$ are the statistical parameters pertinent to the matrix; σ_{M} represent the stresses acting on the matrix.

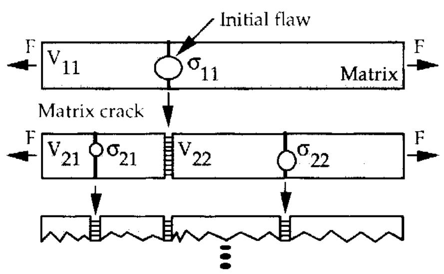

Figure 1. Schematic diagram showing the formation of matrix fragments.

Debonding caused by deflection of the matrix cracks into the interphase affects locally the applied stress-field, inducing stress gradients in the matrix adjacent to the debond. Incorporating the appropriate equations for σ_M, and performing integration of equation (1) gives:

$$P_{Mi} = 1 - \exp\left[-2S_M \cdot \left(\frac{\sigma}{\sigma_{0M}} \cdot \frac{a}{V_M \cdot (1+a)}\right)^{m_M} \cdot \left[l_i - \frac{l_{di}}{m_M + 1} \cdot (m_M + \beta)\right]\right], \quad (2)$$

where l_{di} is the debond length in this ith matrix fragment.

Matrix multiple cracking was then modelled as follows. A given fragment fails when its strength becomes smaller than the stress acting on the matrix. The fragment strengths depend on the fragment sizes. Fragment size is dictated by the location of failure at a previous step. It is derived from the probability of location of the critical flaw. The fragment strength (σ_M^i) derives from the probability of fragment failure.

$$\sigma_M^i = \sigma_M^R \left(\frac{V_{0M}}{V_i}\right)^{1/m_M} \left(1 - \frac{l_{di}}{l_i} \frac{m + \beta}{m + 1}\right)^{-1/m_M}, \quad (3)$$

where σ_M^R is a reference matrix strength for the volume V_{0M} of matrix. V_i is the fragment volume, l_{di} is the debond length, $2l_i$ is the fragment length, $\beta = l_0/l_{di}$ where l_0 is a reference distance along which the Poisson effect is operative.

2.2. *Fracture of fibers*

The fracture of fibers involves the following features seen on SiC/SiC and C/SiC composites and minicomposites during tensile tests: (i) the individual fiber breaks occur at high loads near ultimate failure; and (ii) the fibers fail only once.

After saturation, the crack spacing distance is generally a few microns scale whereas the debond extends along the entire fibers. The load carrying capability of the matrix is tremendously reduced or annihilated. Once a fiber has broken anywhere in the gauge length of the specimen, it is no longer capable of carrying the load [4, 5].

Probability of failure for the fibers is determined by the stress state induced by the matrix cracks and also by the law of load sharing among the surviving fibers, as fibers fail individually. A global load sharing was assumed, as observed in fiber bundles. The failure probability was expressed in terms of an equivalent fiber length (denoted L_{equi}) defined as the length of a fiber subjected uniformly to the peak stress σ_{max}^f for the same failure probability. Failure probability for a fiber within the minicomposites is given by the following equation:

$$P = 1 - \exp\left[-A_f L_{equi}\left(\frac{\sigma_{max}^f}{\sigma_{0f}}\right)^{m_f}\right], \quad (4)$$

where

$$\sigma_{\max}^{\mathrm{f}} = \frac{F}{A_{\mathrm{f}}^{\mathrm{t}}(1-\alpha)}, \tag{5}$$

F is the applied force, A_f is the cross-sectional area of a single fiber, A_f^t is the total cross sectional area of all the fibers present in the minicomposites, m_f and σ_{0f} are the statistical parameters pertinent to the fibers, and α is the fraction of individual fiber breaks. α represents the failure probability of the Nth fiber. The number of fibers N that are broken under a given force F is related to the initial number of fibers N_0 by the following equation:

$$N = N_0 P. \tag{6}$$

Inserting the expression for P into equation (6) the fraction of surviving fibers is given by:

$$q = 1 - \alpha = \exp\left[-A_{\mathrm{f}} L_{\mathrm{equi}}(\alpha)\left(\frac{F}{A_{\mathrm{f}}^{\mathrm{t}}(1-\alpha)\sigma_{0\mathrm{f}}}\right)^{m_{\mathrm{f}}}\right]. \tag{7}$$

The ultimate failure results from an instability in the evolution of individual fiber failures. It is characterized by the following criterion:

$$\frac{\delta F}{\delta \alpha} = 0. \tag{8}$$

2.3. Prediction of the mechanical behavior of minicomposites

Minicomposite deformations are dictated by the fibers. They were derived from the stress field operating on the fibers, as a function of the number of matrix cracks and the fraction of broken fibers (α). The properties required for the computations are given in Table 1.

The force–strain curves predicted for the SiC/SiC minicomposites compared fairly well with the experimental data (Fig. 2). The model allowed determination

Table 1.
Mean characteristics of the SiC/SiC minicomposites

V_f (%)	31.5
V_m (%)	61
Fiber Young's modulus (GPa)	200
Matrix Young's modulus (GPa)	400
Statistical parameters	
matrix: m_M	6.08 (1.66)
matrix: σ_{0M} ($V_0 = 1$ m^3) (MPa)	10.51 (1.23)
fiber: m_f	5.45
fiber: σ_{0f} ($V_0 = 1$ m^3) (MPa)	19.5
τ (MPa)[1]	115

[1] hysteresis loops.

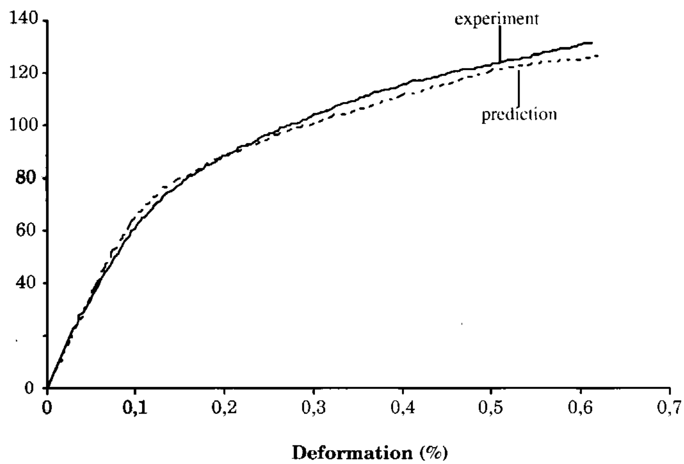

Figure 2. Comparison of the predicted and experimental mechanical behaviors for a SiC/SiC minicomposite.

of the influence of constituent properties on the response of minicomposites. It was shown that the matrix influence is similar to that of the interfacial shear stress. Low stresses and a plateau-like domain are enhanced by a matrix displaying a low strength, a high Weibull modulus and a high Young modulus. Variability in fiber strength causes a significant scatter in the minicomposite strain-to-failure. Finally, it was shown that the minicomposites are significantly sensitive to size effects.

3. PREDICTION OF DAMAGE EVOLUTION IN A 2D WOVEN COMPOSITE

In the composites reinforced with fabrics of fiber bundles the matrix damage is influenced by the microstructure [10]. The 2D SiC/SiC made by Chemical Vapor Infiltration (CVI) display a highly heterogeneous microstructure consisting of woven infiltrated tows that behave as physical entities, large pores (referred to as macropores) located between the plies or at yarn intersections within the plies, and a uniform layer of matrix over the fiber preform (referred to as the intertow matrix). Much smaller pores are also present within the tows. Extensive inspection of the composite under a tensile load using a microscope has shown that matrix cracking affects first the intertow matrix, then the transverse infiltrated tows and finally the longitudinal infiltrated tows [10].

3.1. Determination of failure probabilities

The matrix damage evolution in a 2D SiC/SiC composite was predicted using a finite element analysis of failure probabilities (Fig. 3) [8, 11]. First, the stresses in the matrix are computed using a finite element code (MARC produced by MARC analysis). Then, failure probabilities are determined using the FLAG post processor [8, 11]. FLAG uses the finite-element output (principal stresses), and a material data

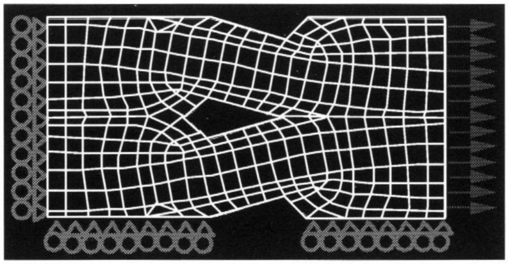

Figure 3. Cell and finite element mesh used in the analysis.

file including the statistical parameters pertinent to composite basic constituents. The FLAG program includes the multiaxial elemental strength model [1, 12] for handling multiaxial fracture statistics. The multiaxial elemental strength model was developed to predict the failure of ceramic materials under various stress-states and geometries. It is based upon the premise that the pre-existing flaws in the material can be characterized by their flaw extension stress, or strength S (referred to as the elemental strength). The flaw distributions are thus described by the distribution in elemental strengths S. The failure probability is then derived from the distribution in S.

The failure probability of a volume element of matrix (i.e. a single finite element mesh unit) is calculated using the following equation:

$$P_V = 1 - \exp\left[-\int_V \left(\frac{\sigma_1}{\sigma_{0V}}\right)^{m_V} I_V\left(m_V, \frac{\sigma_2}{\sigma_1}, \frac{\sigma_3}{\sigma_1}\right) \mathrm{d}V \right], \tag{9}$$

where P_V is failure probability, σ_1, σ_2 and σ_3 are the principal stresses ($\sigma_1 > \sigma_2 > \sigma_3$), m_V and σ_{0V} are the flaw strength parameters, V is the volume of the considered matrix element. The function I_V $(\cdots)$ is detailed elsewhere [1]. It depends upon the local principal stress field through a non-coplanar strain energy release rate criterion for crack extension [1, 12].

3.2. Principle of matrix cracking simulation

The applied deformation (or the applied stress) is increased incrementally. At each increment, the stress-state and the unit mesh failure probabilities are computed. A crack in the intertow matrix or in the matrix in the transverse tows (perpendicular to the loading direction), or a damaged zone in the matrix in the longitudinal tows (parallel to the loading direction) is introduced at the location of the maximum unit mesh failure probability when this computed failure probability reaches the value of 1, in order to represent definite events. The cracks are introduced in the mesh by iteratively splitting the nodes. The damaged zones are characterized by an effective Young's modulus according to the density of matrix cracks, in order to take into account the contribution of the debonded fibers in the deformations of these longitudinal tows.

3.3. Application to a 2D SiC/SiC composite

The properties of constituents required for computations are summarized in Tables 2 and 3.

A cell of 2D SiC/SiC composite under uniaxial tension was examined first. The damage evolution predicted was found to be in excellent agreement with that identified on practical 2D woven SiC/SiC composites under a uniaxial tensile load (Table 4). The predicted stress–strain curves and Young's modulus compared satisfactorily with experimental data (Fig. 4).

However, a certain discrepancy was observed which was attributed primarily to the matrix/tow interactions.

Then, this approach was applied to predict the damage evolution and the stress–strain behavior of a fully dense 2D woven SiC/SiC composite. The results indicated that the macropores have a beneficial effect on the mechanical behavior (Fig. 5). The short macropore-induced cracks are less detrimental than the long transverse cracks that would appear in the fully dense SiC/SiC.

Finally, the potential of this approach to handle complex loading conditions was illustrated on a cell subjected to non-uniform forces. The approach predicted the damage evolution (involving intense debonding) observed on practical CMCs

Table 2.
Main mechanical properties of composite constituents

Constituents	Young's modulus (GPa)	Poisson's ratio
Fiber	200	0.25
Matrix	400	0.20
Longitudinal tows	260	0.20
Damaged longitudinal tows	100	0.25
Transverse tows	160	0.20

Table 3.
Statistical parameters of the SiC matrix in the different constituents of the SiC/SiC composite

Constituents	Weibull modulus	Scale factor (MPa)
Microcomposite	4.9	1.6
Minicomposite	6.2	11.3
Interply matrix	4.9	1.6
Transverse tow matrix	4.9	0.66
Longitudinal tow matrix	6.2	7.3

Table 4.
Comparison of the predicted evolution of matrix damage with experimental results in a 2D SiC/SiC composite under uniaxial tension

Prediction		Experiment	
deformation ε (%)	damage	deformation ε (%)	observed damage
0.04	crack initiation at macropore singularities	0.035	crack initiation at macropore singularities
0.11	cracking in transverse tows	0.085	cracking in transverse tows
0.2	cracking in longitudinal tows	0.185	cracking in longitudinal tows

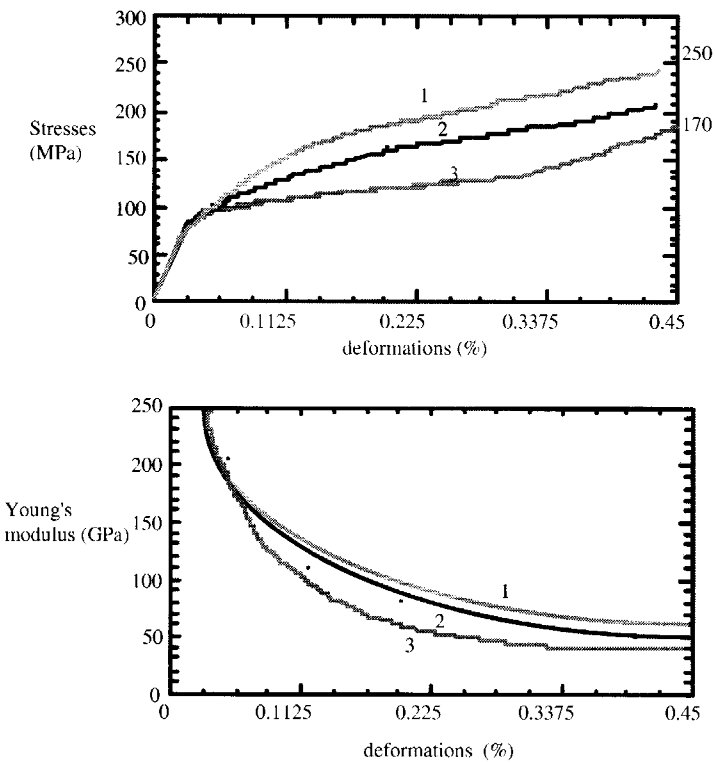

Figure 4. Comparison of experimental (1) and predicted (2), (3) stress–strain behaviors and Young's moduli: (2) [13]; (3) present analysis.

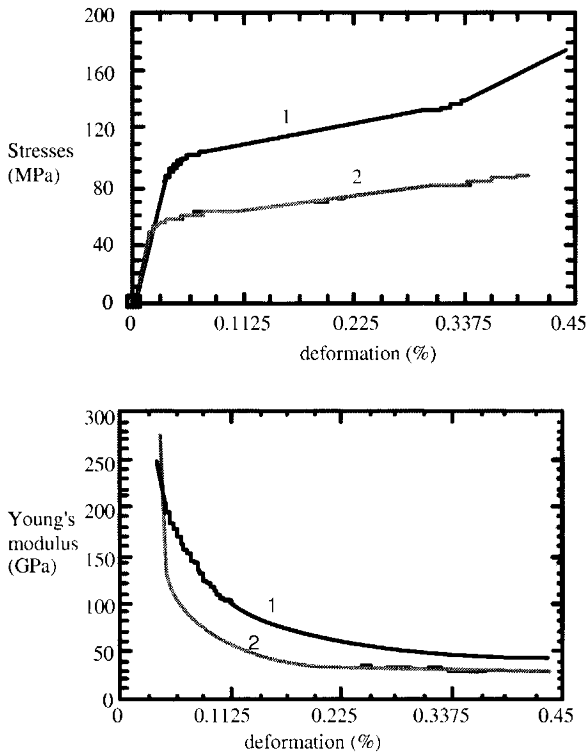

Figure 5. Comparison of the stress–strain behaviors and the Young's moduli predicted (1) for the conventional 2D SiC/SiC composite, and (2) for the corresponding fully dense 2D SiC/SiC.

under bending conditions. The stress–strain curve exhibited the features of the mechanical behavior evidenced on the practical 2D woven SiC/SiC composite subject to bending.

4. CONCLUSIONS

The model of the force–strain behavior of minicomposites which was presented is based on a probabilistic-statistical description of matrix cracking and fiber bundle failure. The minicomposites are assimilated to fiber bundles subjected to a typical stress-state induced by the presence of matrix cracks and associated debonding. A Weibull type statistical-probabilistic model was developed for the description of the matrix cracking process and fiber failure. This model provided stress-probability equations as a function of the number of matrix cracks and various constituent properties.

The force–strain behaviors that were predicted from the characteristics of constituents were in excellent agreement with the experimental ones, thus validating the model. Important trends in the influence of constituents properties on the mechanical behavior of minicomposites were anticipated.

The damage evolution, which was predicted from properties of basic constituents using failure probability computations, was found to be in excellent agreement with that identified on practical 2D woven SiC/SiC composites. The predicted stress–strain curves and Young's modulus compared satisfactorily with experimental data. However a certain discrepancy was observed which was attributed primarily to the matrix/tow interactions.

Then, this approach was applied to a fully dense 2D woven SiC/SiC composite. The results indicated that the macropores have a beneficial effect on the mechanical behavior. Finally, the potential of this approach to handle complex loading conditions was illustrated on a cell subjected to non-uniform forces. The results indicate that this approach may be used to simulate matrix damage and related stress–strain behavior of CMCs from properties of basic constituents.

Acknowledgements

This work has been supported by the Ministry of Education and Research, CNRS and SEP. The author acknowledges the contribution of former students including L. Guillaumat, N. Lissart, B. Thommeret and Ch. Percevault.

REFERENCES

1. J. Lamon and A. G. Evans, *J. Am. Ceram. Soc.* **66**, 177 (1983).
2. W. A. Curtin, *J. Am. Ceram. Soc.* **74**, 2837 (1991).
3. P. S. Steif and H. R. Schwietert, *Ceram. Eng. Sci. Proc.* **11**, 1567 (1990).
4. M. Sutcu, *Acta Metall.* **37**, 2567 (1989).
5. H. Cao and M. D. Thouless, *J. Am. Ceram. Soc.* **73**, 2091 (1990).
6. L. Guillaumat and J. Lamon, *Int. J. Fract.* **82**, 297 (1996).
7. N. Lissart and J. Lamon, *Acta Metall.* **45**, 1025 (1997).
8. J. Lamon, B. Thommeret and C. Percevault, *J. Eur. Ceram. Soc.* **18**, 1197 (1998).
9. J. Lamon, N. Lissart, C. Rechigniac, D. M. Roach and J. M. Jouin, *Ceram. Eng. Sci. Proc.* 1115 (1993).
10. L. Guillaumat and J. Lamon, *Revue des Composites et des Matériaux Avancés* **3**, 159 (1993).
11. J. Lamon and B. Thommeret, *Ceram. Trans.* **57**, 77 (1995).
12. J. Lamon, *J. Am. Ceram. Soc.* **73**, 2204 (1990).
13. L. Guillaumat and J. Lamon, *Compos. Sci. Technol.* **56**, 803 (1996).